American Journal of Engineering Research (AJER) ***2017***
American Journal of Engineering Research (AJER)
e-ISSN: 2320-0847 p-ISSN : 2320-0936
Volume-6, Issue-9, pp-97-105
www.ajer.org
Research Paper Open Access

Study of Surface Crack Growth in Railway Wheels With Fairly Small Plasticity

[1]Azade Haidari, [2]Mojtaba heidari
[1]*PhD student of IRAN University of science and technology*
[2]*Masters student of Isfahan University of technology*
Corresponding Author: Azade Haidari

ABSTRACT: *This paper provides a method for addressing surface crack growth in railway wheels, taking into account rail and brake blocks effects. A 3D elastic-plastic finite element model has been used to perform the thermo-mechanical analysis of wheel. The importance of axle load, speed, plasticity and braking thermal load on growing of a surface crake situated on a tread of railway wheels are studied in this paper. For this purpose a FE model of a wheel, with two brake shoes and a portion of rail are created and realistic loads and boundary conditions, are applied to the model. It is assumed that the wheel has contained a surface semi-elliptical crack on its tread surface. In this article the effects of thermal loads of braking, elastic-plastic model, rotating speed of wheel and axle loads on the stress intensity factors are studied and the obtained results show the importance of these factors while in the most of available papers only rolling contact is studied.*

Keywords: *Railway wheel, surface crack, thermo-mechanical analysis, plasticity*

Date of Submission: 13 -05-2017 Date of acceptance: 20-07-2017

I. INTRODUCTION

The wheel is one of the key components on train and its failure may cause serious accident especially in high speed and heavy haul railway. Derailment due to wheel failure would cause a tremendous social and economic cost in service operation. It is necessary to evaluate the safety of railway wheel by calculating quantitatively the fracture limit and remnant life of cracked railway wheels under service loads. The surface damage of wheel materials plays a fundamental role in determining the operational reliability of railway systems and based of Kwon et al. (2012) one of the most common damage case generated in railway wheels is surface semi-elliptical crack which is studied in this paper. Caprioli (2015) studied short rolling contact fatigue and thermal cracks under frictional rolling but her study did not include the hardening, axle load and speed.

However, rolling contact loads in rail-wheel contact region create the greatest mechanical stress fields; other loads, such as friction force between rail and wheel, brake pressure and thermal loads of braking, affect stress and strain fields of the wheel too while in Peng et al. (2012) and Peng et al. (2013) studies on the railroad wheels effects of these factors were ignored. Based on our studies effects of above parameters are non-negligible. Nowadays by increase of train speeds and axle loads, having a deeper knowledge to prediction of fracture life of cracked wheels is an important problem which is studied in this article. Here a fatigue crack propagation prediction model based on fracture mechanics method using the results of FE model is investigated and effects of axle load speed and hardening (elastic- plastic) is studied.

II. MATERIAL AND METHODS

Observations show that the size of axle load and the values of wheel strain from the rail at brake application affect the wheel damage and therefore are studied in this article. Moreover, the heating of brake application and the thermal stress at the cooling process may become an important stress source in crack growth [1]. In many of articles, effect of friction between the wheel and rail during contact and the contact region stress, which promote plastic deformation in the tread surface, have not been considered. Further, the effect of combined thermal and mechanical loads on a three-dimensional model has not been addressed and Hertz theory has been used to calculate wheel/rail. Using the Hertz contact theory for 2D elastic model show the acceptable results but in 3D models with elastic-plastic property, one of the reasons for non-compliance the experimental with theoretical results is Hertz theory. In this article we're going to three dimensional modelling of rail, cracked wheel and brake blocks and simulation the conditions closer to reality, the effects of thermal loads of braking

and hot spot generated as its result, plastic deformation during the operational cycles, axle load and rotating speed of the wheel, studied.

2.1. Tread thermal loads

The braked wheel tread is subjected to periodic (with wheel revolution) heating and cooling which leads to significant temperature variations and thus create high thermal stress and strains. Therefore thermal loads of braking and its associated stress and strains can contribute to surface crack nucleation and growth. At near the surface the thermal skin experiences significant periodic thermal variations owing to the recurring pulses of brake friction heating, rail chilling and convection losses. These periodic changes in surface temperatures are usually ignored in wheel thermo-mechanical analyses. Nevertheless, such periodic temperatures can be important factors in surface failure of wheels [4].

In this paper, thermal behaviour of the block-wheel–rail system will be studied to determine the temperature fields in them. Some phenomena such as thermo-mechanical block-wheel contact, rail-wheel slip at braking process, wheel rotation, are not included in the most available articles. We could find no references that addressed the effect of combined thermal and mechanical loads (axle load, rail-wheel contact friction, wheel rotation, brake pressure, heat generation during brake applications and heating and cooling of all parts due to conduction and convection heat transmission) on the crack growth of the wheel by 3D modelling of rail, wheels and brake blocks.

2.2. Finite element method

To build a realistic model and obtain more accurate results, a 3D elastic-plastic finite element model is used. This model should be able to accurately calculate the 3D state of strains and stresses in the contact region of rail-wheel and wheel-blocks. Here, *Abaqus 6.11* is used for these purposes. At this FE method heat partitioning factors are applied to wheel-rail and wheel-blocks contact. By using appropriate boundary conditions, dissipation of heat to the surroundings by convection is accounted in presented model too. In order to obtain the mechanical stress fields due to rail-wheel rolling contact and also thermal stresses created at braking stage, two cast iron brake blocks and the wheel, that rotates on a portion of a rail (the length of rail is considered equal to distance between two sleepers), are modeled. The angular velocity of wheel is equal to *50rad/s*. The model of wheel- rail- block used in this article is shown in Fig 1. (a).

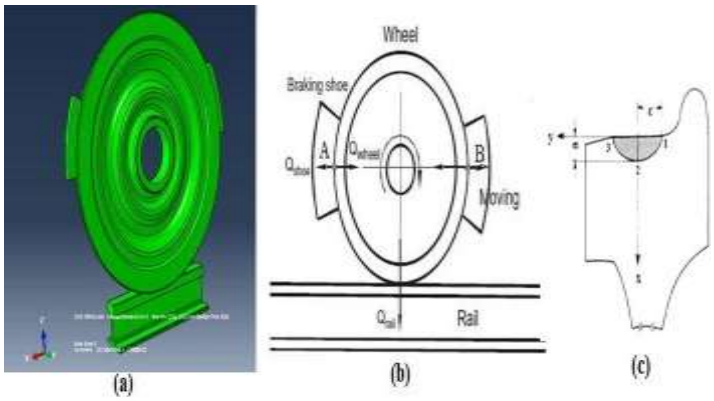

Fig. 1.(a) 3D finite element model of rail-wheel- brake blocks system. (b) 2D view and a schematic model of the crack position measurement. (c) schematic view of semi-elliptical crack.

The frictional power generated during a brake cycle is assumed to be transformed into frictional heat at the contact area, i.e. over the common area of contact between block and wheel. For determining temperature rise of all components (rail, wheel and brake shoes); it is necessary to define a parameter as the heat partition factor [5], which describes what portion of heat generated in contact region of two bodies, is transferred to each of them. This quantity in the rail-wheel and wheel-block contact area is explained in [6]. The brake blocks are modelled as cast iron blocks and proper thermal and mechanical properties are considered for them. Also the brake block configuration used in this article is: *2Bg* (two blocks per two holders).

A finite element analysis (FEA) has been employed to study 3-D semi elliptical surface crack in the railway wheel. This wheel is subjected to angular velocity of 50rad/s, axle load of 145KN and rail-wheel contact shear and normal stresses in the first step of analysis. While in the second step, two cast iron brake shoes compress to the wheel tread surface with braking pressure of 700MPa and generate high friction in the contact zones and also cause to occurrence of slip of the wheel on the rail surface. By considering accurate mechanical and thermal properties of wheel, rail and brake shoes and applying proper loads and boundary conditions, the

crack behaviour under thermo-plastic conditions can be achieved. Fig 1. (b) shows a 2D view of model. The time step considered in this study is equal to time to one revolution of the wheel. At the start of step, the crack is in contact region of wheel with the left brake block and during a full rotation at the end of the step again returns to the left block-wheel contact zone. Thus according to rotational speed of wheel (50rad/s) any increment of step time is corresponding to an angular position of the crack compared to its initial position. Graphical presentation of rail, wheel and brake blocks is shown in Fig 1. (b). From this Fig and according to direction of wheel rotation, crack position can be measured by any angle between the radius passing from the crack and line AB. In the following, all crack positions measured compared to this line.The crack considered in this paper is a semi-elliptical surface crack with semi-minor and semi-major axis of 5 and 7mm respectively. This crack is shown in Fig 1. (c).

III. IMPORTANCEOF HOT SPOTS

At braking, as the wheel rotates, different points of tread surface, experience both heating and cooling. The conditions at the two thermal contact interfaces which are associated with the wheel–rail and brake–wheel interfaces are complex and hot bands and/or hot spots may develop within the contact regions and they may lead to a highly non-uniform heat production and resulting temperature concentration and high thermal strains and stresses.

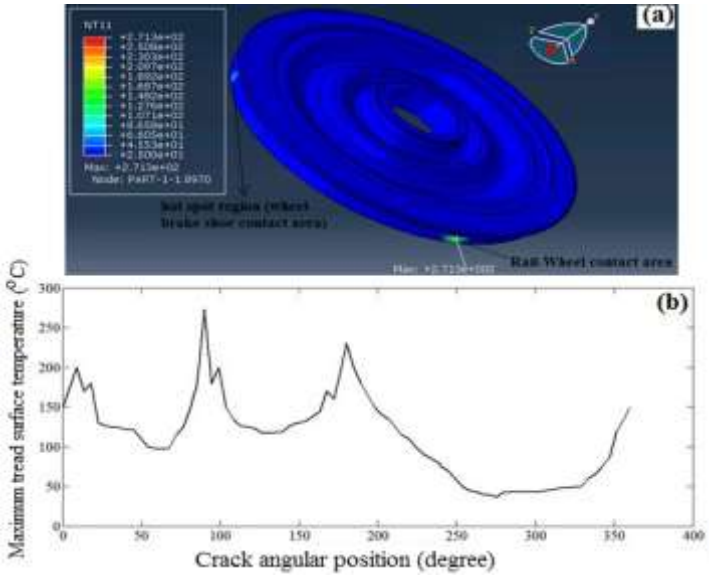

Fig 2. (a) Temperature field of tread surface of wheel for ω=50rad/s. (b) Variation of maximum tread surface temperature for different crack positions.

In many of papers, by considering a thermal band with average braking power, effect of thermal loads of braking is considered but this method doesn't contain the hot spots created due to contact between rolling wheel tread surface and brake blocks. These hot spots have the considerable higher temperatures compared to surrounding surface and make the first contact with brake shoes on brake applications and they have considerable roles in fatigue (crack initiation) and crack growth of railroad wheels. Due to the non-uniform heat flow, different points of wheel will experience their extreme values of the temperature field at different times. It is assumed that, before braking occurs, all of parts (rail, wheel and brake shoes) are at uniform reference temperature $T_0=25^oC$ [7]. Wheel temperature field obtained from thermal analysis of used 3D model embraces the hot spots due to brake shoes modeling and is shown in Fig 2. (a).

IV. MODEL AND CALCULATION

The linear hardening model for wheel and rail is used in this study. Mechanical and thermal properties of brake blocks are adopted correspond to cast iron blocks. Rail and the wheel are made of steel grade *R7T* with hardness properties that is mentioned in Table 1.

Table 1. Linear isotropic hardening properties of steel *R7T*.

Plastic stress (MPa)	Plastic strain
545	0
763.625	0.02099
887.25	0.0445
958.125	0.0863

Referring to the coordinate axes "*x*", "*y*" and "*z*" in Fig 1. (c), the stress components of interest are "σ_{zz}", "σ_{xz}" and "σ_{zy}"; they would exert mixed mode effects on crack growth. Assessment of mixed mode cracking would be made for each point on the crack front by referring to the stress "σ_{zz}" normal to the crack plane and "σ_{zy}" and "σ_{xz}" parallel to the crack surface [9]. According to fracture mechanics laws, LEFM can be used until the plastic zone size around the crack be negligible compared to the crack dimensions. Therefore the usability of calculating stress intensity factors (K_I, K_{II} and K_{III}) as fracture parameters is studied in this section. For this purpose, the von Mises stress contour around the crack is shown in Fig. 3. based on values of Table 1, plasticity occur at stresses higher than 545MPa which in presented model, theses stress values Only seen in areas shown in red in the this Fig and its size is about 0.5mm which is smaller than maximum allowable plastic zone size for using LEFM (The maximum radius of plastic zone is allowed to LEFM and stress intensity factors is equal to1/8 crack length) therefore in this study K factors as a measure for crack intensity effect can be used. The general crack propagation function is expressed as Eqn. (1):

$$\frac{da}{dN} = C\left(\frac{\Delta K_{eff}}{(1-R)^{\zeta}}\right)^{m} \quad (1)$$

Where *da/dN* is the crack growth rate, ΔK_{eff} is the effective stress intensity factor range for mixed-mode loading, Ris the stress ratio (-1≤R≤1) and *C*, *m* and ζ are material parameters. For the data reported by Kuna et al. [10], *C*, *m* and ζ are determined by regression analysis as $5.8e^{-9}$, 2.95 and 1, respectively. R is stress ratio of crack tip (proportion of maximum to minimum stress intensity factor) and according to Figs 6-8 which will be presented in the following, its values for all three modes are nearly -1 and therefore here R=-1 is used.

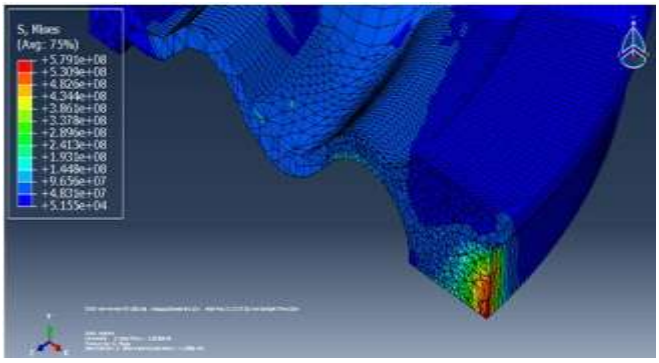

Fig. 3. Maximum plastic zone size of the crack.

In this paper the stress intensity factor is evaluated directly based on displacement discontinuities using a three-dimensional finite element model which is presented in Eqns. (2-4) [11].

$$K_I = C\frac{D_n E\sqrt{\pi}}{4(1-\nu^2)\sqrt{P}} \quad (2)$$

$$K_{II} = C\frac{D_S E\sqrt{\pi}}{4(1-\nu^2)\sqrt{P}} \quad (3)$$

$$K_{II} = C\frac{D_t E\sqrt{\pi}}{4(1-\nu^2)\sqrt{P}} \quad (4)$$

Where *"E"* is modulus of elasticity, "*ν*" is Poisson's ratio and *"P"* is crack tip element length perpendicular to crack front. In presented FE model the length of crack tip element (*P)* is equal to 0.6mm. *"D_n"* is the opening displacement discontinuity of crack tip element, *"D_s"* is shear displacement discontinuity perpendicular to "D_n" and the crack front, *"D_t"* is front-parallel displacement discontinuity. *"C"* is an empirically determined constant that accounts for the discrepancy between the numerical approximation and the analytical solution and according to [11] *C* = 0.806 is used here.In presented mixed-mode crack growth, all SIFs for different modes are combined using Eqn. (5), which calculated equivalent SIF *($K_{mixed,eq}$)* [12]:

$$K_{mixed,eq} = \frac{1}{B}\sqrt{(K_I^2 + (\frac{K_{II}}{s})^2 + (\frac{K_{III}}{s})^2 + A(\frac{K^H}{s})^2} \quad (5)$$

In this equation, material parameter *"s"* is related to the material ductility, *"A"* and *"B"* are material parameters and superscript *"H"* indicates the hydrostatic stress related term. These parameters and their values are explained in [12]. Eqn. 1 can be written as a separable statement and the number of required cycles for initial crack in wheel to attain the critical size may be obtained as:

$$N(a) = \frac{1}{C(\Delta F)^m}\int_{a_0}^{a_c}\frac{(1-R)^{\zeta m}\,da}{\sqrt{\pi a}\,Y(a)^m} \quad (6)$$

Where "ΔF" is the applied vertical loading range and *"Y(a)"* is a geometry function considering the effect of crack configuration and boundary conditions and ignoring it may be a non-negligible source of error. Therefore we use the following equation [12]:

$$\Delta K_{eq} = \Delta S_{eq} Y\sqrt{\pi a} \quad (7)$$

By putting the obtained stress intensity factors from Eqn. (5) in Eqn. (7) and assuming a constant equivalent stress (ΔS_{eq}), Y(a) is obtained as a function of major diameter length of crack (a) for any crack increment. Among many of the proposed fracture criteria, the strain energy density criterion or S-theory developed by Sih is one of the most expedient criterions for crack growth direction predicting. When all three stress intensity factors are present, they could be combined into the strain energy density factor as:

$$S = a_{11}K_I^2 + 2a_{12}K_I K_{II} + a_{22}K_{II}^2 + a_{33}K_{III}^2 \quad (8)$$

$$a_{11} = \frac{8E}{\pi(1+\nu)}(3 - 4\nu - cos\theta)(1 + cos\theta) \quad (9)$$

$$a_{12} = \frac{16E}{\pi(1+\nu)}sin\theta(cos\theta - 1 + 2\nu) \quad (10)$$

$$a_{22} = \frac{8E}{\pi(1+\nu)}[4(1-\nu)(1-cos\theta) + (3cos\theta - 1)(1 + \cos\theta)] \quad (11)$$

$$a_{33} = \frac{32E}{\pi(1+\nu)} \quad (12)$$

"E" and "ν" are the Young's modulus and Poisson's ratio respectively. The angle "θ" is measured in the plane normal to the crack border. That is, *"$\theta = 0$"* would correspond to the *xy*-plane in Fig 2.(c). Direction of crack growth, (θ_0) for a point on the crack border, would depend on the relative magnitudes of the three stress intensity factors K_I, K_{II} and K_{III}. considering S-theory the crack grows in the direction determined by the relative minimum of the strain energy density factor S (S_{min}) So the condition $\partial S/\partial\theta=0$ and $\partial^2 S/\partial\theta^2 > 0$ is used for determination of crack growth direction. The crack growth would occur till K_{eq} reaches to critical value K_{IC}. In this work, the considered value of K_{IC} for railway wheel is $85MPa\sqrt{m}$ [13].

By considering the original semi elliptical crack on the *xy* plane and calculating stress intensity factors components (K_I, K_{II} and K_{III}), the first crack increment direction is calculated by minimizing S factor. The results obtained for crack growth direction and stress intensity factors for original crack in mechanical and thermo-mechanical analyses are listed in Table 2.

Table 2. Results of presented FE model for the original crack (ω=50rad/s).

	KI (MPa√m	KII (MPa√m)	KIII (MPa√m)	Keq (MPa√m)	θ0
Mechanical analysis	2.83	0.61	1.661	4.128	11°
Thermo-mechanical analysis	4.8	1.7	1.81	6.397	~0°

According to presented results, stress intensity factors obtained from thermo-mechanical analysis are considerable greater than corresponding values of mechanical analysis and hence the importance of thermal loads of braking is obvious. In Table 2 the results of first increment of crack growth are shown. Crack growth estimation is a long and repetitive procedure so that after determining the first crack direction (θ_0), the new crack plane with an increment in its size is modelled and SIFs and θ_0 for new crack are calculated and this process continuous till the value of K_{eq} reaches to wheel material toughness (K_{IC}).

The variations of crack growth direction *"θ_0"* during crack growth analysis are shown in Fig. 4 for mechanical and thermo-mechanical model. As can be seen from this Fig, for the initial increments, *"θ_0"* has a small value (θ_0~11° for mechanical and θ_0~0° for thermo-mechanical analysis) and over time, its value increases such that reaches to 65° and 72° for mechanical and thermo-mechanical analyses respectively. This is an acceptable result from [9] which states Initially, K_I is more dominant and the crack grew in the original plane nearly. The influence of shear stresses (σ_{xz}, σ_{yz}) and their corresponding stress intensity factors (K_{II}, K_{III}) increases as crack grows in presented FE analyses which is similar to experimental results where an out-of-plane crack growth orientation angle of $\theta_0 \sim 80°$ is observed.

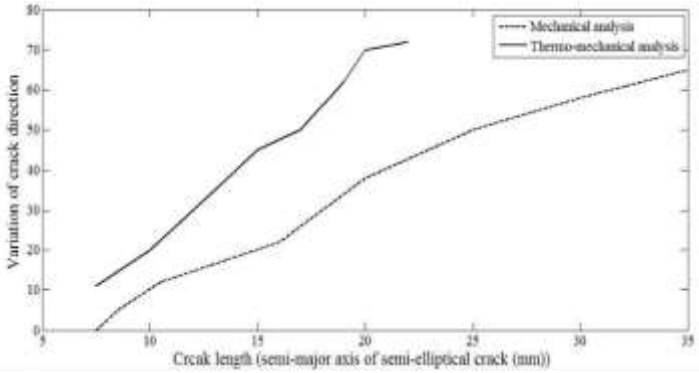

Fig4. Crack growth direction and critical length of mechanical and thermo-mechanical analysis.

The fracture life of the wheel for presented mechanical analysis is about 1.2×10^6 cycles and has acceptable accordance with results of [1] for initial flaw size of 5mm while by considering the thermal loads effect (thermo-mechanical analysis) the fracture life decrease to 0.7×10^6 cycles which shows the non-negligible effect of thermal stresses on the crack growth of wheel. On the other hand, the critical crack size is obtain equal to 33mm which has a good accordance with the result of mechanical analysis of [1] (a_c=35mm).

V. RESULTS AND DISCUSSION

4.1. Axle load effects

In recent years by increasing demands for high speed services and higher axle loads, new challenges with respect of fracture life of cracked wheels and their safety issues are created [14]. So In this paper, axle load as one of the factors affecting wheel damage is studied and also effect of speed increase is investigated. In this section, analyses are done for three different vertical loads (*58.5 kN, 102.3 kN,146.2kN,*) and effects of axle load are studied. Maximum tread temperature and mechanical and thermo-mechanical K_{eq} of the wheel for these three axle loads are listed in Table 3.

Table 3. Effect of axle load on the results.

	Max tempraturte	Keq(mechanical)	Keq (thermomechanical)
58KN axle load	150	1.7	2.9
102KN axle load	203	2.8	3.9
146KN axle load	271.3	4.13	6.4

As can be seen from results shown in this table, by axle load variation, maximum temperature of wheel tread surface changes too. The results show that a higher axle load, gives a higher temperature so the importance of braking thermal loads increases for heavier trains. The sliding between wheel and rail can generate a very high temperature and would cause serious friction damage to wheel and rail. So with increasing axle load, the frictional sliding increase and as a result, higher values for maximum temperature of tread surface will be obtained. Studies of Chuanxi et al. [15] shown thermal damage of wheel (due to wheel sliding) can be more serious for heavy haul and high speed railway and therefore the need of thermo-mechanical analysis of wheel specially for these two cases (higher axle load and velocity) appears.

The variation of equivalent stress intensity factor with axle loads are calculated for the both mechanical and thermo-mechanical analyses and illustrated in Table 3 too. The results demonstrates that by increasing axle load, mechanical and thermo-mechanical stress intensity factor increase and therefore fracture life of wheel will be reduced. On the other hand, according to presented obtained results, difference between mechanical and thermo-mechanical results for axle load of 102.3KN, is about 26% while for vertical load of 146KN, this difference increases to 36% and so it can be concluded for heavier trains, importance of consideration of braking thermal load, increases.

4.2. Effect of speed increase

The effect of speed on temperature field and SIFs of the cracked wheel in the both case of mechanical and thermo-mechanical analyses, is studied. For this purpose, analyses are done for angular velocity of 100rad/s and the results are compared to results of 50rad/s angular velocity. The results obtained from this study show that the temperature field of wheel is very sensitive to velocity. In addition to temperature, mechanical and thermo-mechanical stresses and strains of the wheel increase due to increase of wheel velocity and therefore the crack growth life of wheel reduces by increase of wheel speed. The mechanical and thermo-mechanical values

of SIFs for angular velocity of 100rad/s for the original crack are shown in Table 4.

Table 4. SIFs values of wheel for $\omega=100rad/s$.

	KI (MPa√m)	KII (MPa√m)	KIII (MPa√m)	Keq (MPa√m)
Mechanical analysis	4.27	1.274	2.16	6.035
Thermo-mechanical analysis	5.81	2.53	2.77	8.621

As can be seen from results of this table, thermo-mechanical results have s deviation from mechanical analysis. On the other hand it may be concluded from comparison of Table 4 and Table 2 that an increase of velocity have a destructive effect on the fracture life of the cracked railway wheel due to increase of SIFs so nowadays because of increase of train velocity and harmful effects of this increase on the fracture life of cracked railway wheels, the crack growth of wheels become a very important issue and should investigate attentively.

4.3. Elastic-plastic material model

Linear-elastic and elastic-plastic responses of equivalent stress intensity factor for thermal and mechanical loads considered in this paper have been compared. It was found that differences between linear elastic and elastic-plastic responses for the semi-elliptical surface crack is considerable and therefore, it can be noted how the hardening model is able to capture the accumulation of plastic strain and changes the fracture life of wheel [16]. By considering plasticity, using the Hertz contact theory gives results with less precision since according to this theory, it is assumed that the materials at contact are elastic while experimental and also presented FE results imply on the non-negligible plastic deformation at contact surfaces and therefore for presented elastic-plastic model, modeling of rail and brake blocks is more important [17]. The excessive plastic deformation at the surface in wheel–rail contact limits the use of Hertz contact theory. The FE analyses show that plasticity is limited in the residual state during load traversals. Based on observations, the stresses formed in the course of braking and subsequent cooling attain the plasticity limit of the rail-wheel steel in tension and compression. Fig 5 shows difference between results of elastic-plastic and linear elastic model which shows maximum value of equivalent stress intensity factor in elastic-plastic model is 1.27 times higher than corresponding value in linear elastic model. So fracture life of wheel by considering plasticity properties of wheel reduces and hence from here, importance of applying hardening features on the model becomes clear. In case of elastic plastic problems, the total strain components is components is equal to sum of the elastic and plastic strains$(\varepsilon_{ij}= \varepsilon^{e}_{ij}+ \varepsilon^{p}_{ij})$ [18]

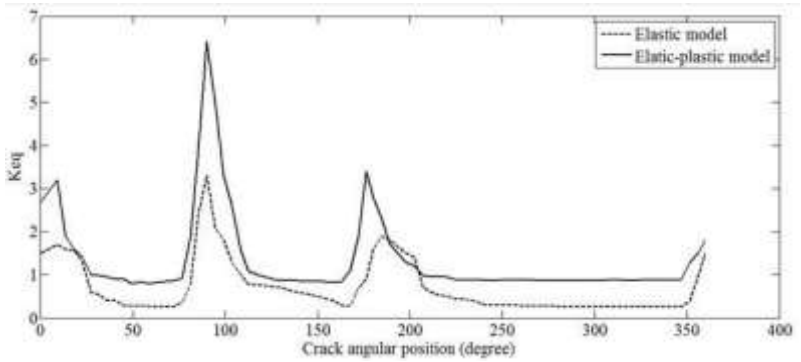

Fig 5. Difference results of elastic-plastic (isotropic hardening) and linear elastic model for wheel.

4.4. Thermal loads effect

The sudden local thermal expansion caused by this pulse temperature increase in a thin surface region is restrained by the relatively cooler surrounding material and create high local stress and strains at contact regions while by considering thermal loads of braking as a uniform thermal band on the wheel tread, which is used in many papers, the results accuracy reduce. The thermal loading cycle that the wheel is subject to through its life results in what is termed a stress reversal within the material. Over time, the cyclic loading causes the residual stress state of the wheel to change from one of compressive stress to tensile stress. This is due to the small amounts of plastic deformation, which occur during each thermal loading cycle. The material is unable to recover from the plastic deformation, caused through thermal expansion when cooling occurs. As cooling occurs from peak temperature down to room temperature, tensile stress occurs on the tread [19]. Variation of KI, KII and KIII for mechanical and thermo-mechanical analyses is shown in Figs 6-8.

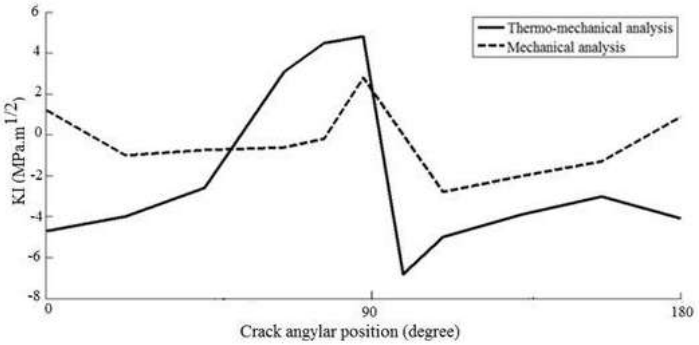

Fig 6. Variation of K_I with crack position.

According to Fig 6, the maximum positive value of K_I for thermo-mechanical analysis is higher than mechanical value. In braking process, a negative traction (mechanical load) applied to the wheel and will induce higher longitudinal stresses (normal stress in rolling direction and normal to crack plane). On the other hand, braking thermal loads during cooling, introduce a tensile stress which will promote subsequent crack growth. As can be seen from this Fig the maximum positive value of "K_I" for thermo-mechanical analysis is considerably higher than corresponding mechanical value. Difference between maximum positive value of mechanical and thermo-mechanical K_I is 41% which is non-negligible.

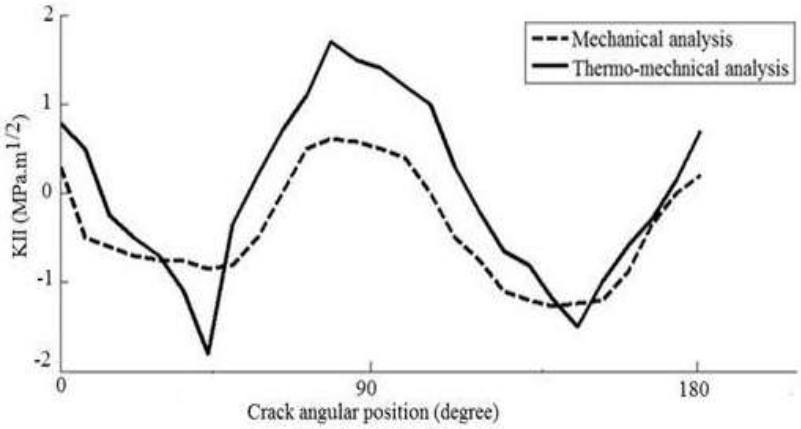

Fig 7. Variation of K_{II} with crack position.

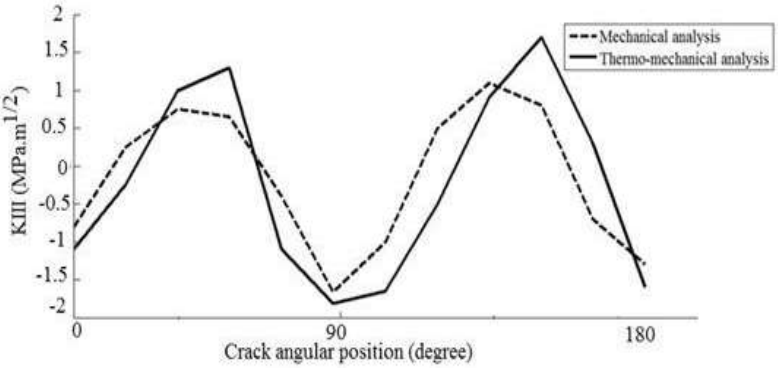

Fig 8. Variation of K_{III} with crack position.

Figs 7 and 8 show variation of K_{II} and KIII for different crack positions. The presence of K_{II} and K_{III} gives rise to out-of-plane crack growth which can be estimated from Eqns. (8-12). It is visible from these two Figs that maximum values of K_{II} and K_{III} for thermo-mechanical analysis is considerably higher than mechanical values which demonstrate the importance of thermal loads on the crack growth. The values of K_{II} and K_{III} increases as the contact loads (rail-wheel and wheel-blocks contact) approaches the crack, and their sign

is reversed when the load has passed over the crack, because the direction of the relative slip of the crack faces is reversed.

VI. CONCLUSION

The semi-elliptical surface crack in a railway wheel is investigated by three dimensional elastic-plastic finite element analyses of a cracked wheel, rail and brake shoes. The results show that:

1- Alternative temperature variations (as imposed by tread braking) on wheels containing surface crack, increase the SIFs magnitude amplitude and reduce the fracture life of wheel.
2- in order to achieve the most accurate and reliable results, considering combined thermal and mechanical loads with exact modeling of wheel, rail and brake blocks is an important issue.
3- Axle load has a considerable effect on creation of thermal loads and traction. On the other hand, as the angular velocity increase, temperature, stress and strain field increase too and therefore the life of wheel reduces. So it can be concluded that the crack growth for higher speeds and heavier trains, becomes more critical and necessitate precise estimation of crack growth life of wheel by considering all thermal and mechanical loads applied to wheel.
4- Considering elastic-plastic behavior by modeling the strain hardening, increase the importance of rail and blocks modeling (instead of using Hertz theory). On the other hand, plastic deformation (in elastic-plastic model) has a destructive effect on remnant life of cracked wheel. If the models assumed to be elastic, SIF components have the lower values and thus longer life will be archived.

REFERENCES

[1]. Kwon, S. J., Lee, D. H., Seo, J. W. and Kwon, S. T., "Safety Margin Evaluation of Railway wheel Based on Fracture Scenarios," International Journal of Railway, 5, No. 2, pp.84-88 (2012).
[2]. Peng, D., Jones, R. and Constable, T., "An investigation of the influence of rail chill on crack growth in a railway wheel due to braking loads," Engineering Fracture Mechanics, 98, pp.1–14 (2013).
[3]. Peng, D., Jones, R. and Constable, T., "A study into crack growth in a railway wheel under thermal stop brake loading spectrum," Engineering Failure Analysis, 25, pp.280–290 (2012).
[4]. Moyar, G, J. and Stone, D. H., "An analysis of the thermal contributions to railway wheel shelling," Wear, I44, pp.117-138 (1991).
[5]. Vernersson, T., "Temperatures at railway tread braking. Part 1: modeling," Proceedings of the Institution of Mechanical Engineers, Part F: Journal of Rail and Rapid Transit, 221, no. 2, pp.167-182 (2007).
[6]. Haidari, A. and Hosseini-Tehrani, P., "Fatigue analysis of railway wheels under combined thermal and mechanical loads," Journal of Thermal Stresses, 37, pp.34–50 (2014).
[7]. Rossmanith, H. P., Loibnegger, F. and Huber, R., "Thermomechanical fatigue fracture due to repeated braking of railway wheels," Materials Science, 42, No. 4, pp.466-475 (2006).
[8]. Tudor, A. and Khonsari, M M., "Analysis of Heat Partitioning in Wheel/Rail and Wheel/Brake Shoe Friction Contact: An Analytical Approach," Tribology Transactions, 49, pp.635-642 (2006).
[9]. Meizoso, A. M., Martinez Esnaola, J.M. and Fuentes Perez, M., "Approximate crack growth estimate of railway wheel influenced by normal and shear action," Theoretical and Applied Fracture Mechanics, 15, pp.179-190 (1991).
[10]. Kuna, M., Springmann, M., Madler, K., Hubner, P. and Pusch, G., "Fracture mechanics based design of a railway wheel made of austempered ductile iron," Engineering Fracture Mechanics, 72, pp.241–53 (2005).
[11]. Sheibani, F., "Solving Three-Dimensional Problems in Natural and Hydraulic Fracture Development: Insight from Displacement Discontinuity Modeling", PhD Thesis, Faculty of the Graduate School of the University of Texas at Austin, Austin, USA (2013).
[12]. Liu, Y., Liu, L. and Mahadevan, S., "Analysis of subsurface crack propagation under rolling contact loading in railroad wheels using FEM," Engineering Fracture Mechanics, 74, pp.2659-2674 (2007).
[13]. Strnadel, B. and Hausild, P., "Statistical scatter in the fracture toughness and Charpy impact energy of pearlitic steel," Material science and engineering, 486, pp.208-214 (2008).
[14]. Zerbst, U., Meadler, K. and Hintze, H., "Fracture mechanics in railway applications—an overview", Engineering Fracture Mechanics 72, pp.163–194 (2005).
[15]. Chuanxi, S., Jun, Z., Chunyan, W. and Xueshan, Z.,"Thermo-Contact Coupling Finite Element Method Analysis of Wheel/Rail Under Sliding Status", International Conference on Information Engineering and Computer Science (ICIECS), Wuhan, China, vol. 1, pp.1–4 (December 19–20, 2009).
[16]. Caprioli, S., "Short rolling contact fatigue and thermal cracks under frictional rolling – A comparison through simulations," Engineering Fracture Mechanics, 141, pp.260–273 (2015).
[17]. Yan, W. and Fischer, F. D., "Applicability of the Hertz contact theory to rail- wheel contact problems," Applied Mechanics, 70, pp.255–268 (2000).
[18]. Debashis, K., Bhushan, A., Panda, S.K. and Biswas, K., "Elastic–plastic dynamic fracture analysis for stationary curved cracks," Finite Elements in Analysis and Design, 73, pp.55–64 (2013).
[19]. Peng, D., Jones, R., Constable, T., Lingamanaik, S.N. and Chen, B.K., "The tool for assessing the damage tolerance of railway wheel under service conditions," Theoretical and Applied Fracture Mechanics, 57, pp.1–13 (2012).

Azade Haidari "Study of Surface Crack Growth in Railway Wheels With Fairly Small Plasticity." American Journal of Engineering Research (AJER), vol. 6, no. 9, 2017, pp. 97-105.